ARMY RESEARCH LABORATORY

Design of a Resistive Susceptor for Uniform Heating During Induction Bonding of Composites

by Bruce K. Fink,
Shridhar Yarlagadda, and John W. Gillespie Jr.

ARL-TR-2148 January 2000

The findings in this report are not to be construed as an official Department of the Army position unless so designated by other authorized documents.

Citation of manufacturer's or trade names does not constitute an official endorsement or approval of the use thereof.

Destroy this report when it is no longer needed. Do not return it to the originator.

Abstract

A novel susceptor concept for metal-mesh susceptors, designed to achieve uniform in-plane temperatures during induction heating, is documented. The process involves redirecting eddy-current flow patterns in the resistive-mesh susceptor by specifically designed cut patterns in the mesh. A theoretical model was developed to predict heat generation in metal-mesh susceptors with any described network pattern. Initial results for cut patterns show significant changes in heating compared to an uncut mesh. Cut patterns can be optimized to reduce temperature gradients in the susceptor to within the processing window of the composite. Experimental results are presented for qualitative comparisons.

Acknowledgments

Research supporting this work was partially funded under the Composite Materials Research Program at the University of Delaware Center for Composite Materials through the U.S. Army Research Laboratory (ARL).

INTENTIONALLY LEFT BLANK.

Table of Contents

INTENTIONALLY LEFT BLANK.

List of Figures

INTENTIONALLY LEFT BLANK.

1. Introduction

Induction heating for nonautoclave or nonoven cure and bonding of composites is a novel approach that may reduce manufacturing costs. Induction heating is an ideal choice for supplying the energy needed for curing thermoset resins and adhesives or for thermoplastic bonding, which is a critical concern in field repair applications. Induction is a noncontact process that can heat geometrically complex parts that are difficult to heat with other bonding methods.

Induction-heated bonding of composites consists of the heating of an interlayer susceptor and the subsequent melting, flow, consolidation, and bonding of two thermoplastic-based adherends or the heating, consolidation, and cure of a thermosetting adhesive. Induction welding of thermoset composites incorporating a co-cured thermoplastic interlayer is also possible [1]. Susceptors may be resistive, for joule heating, or magnetic, for hysteresis heating. For purposes of compatibility, the resistive susceptor can be a metallic screen or mesh (relying on joule heating) embedded in a matrix of the same composition as the composite being welded. The focus of this work is on polymer-impregnated metal-mesh susceptors for use in induction bonding and curing of composites.

Several researchers [2–10] have conducted tests on the use of metal susceptors (in the form of screens or inserts) and resistive heating for bonding of composites. A common problem with metal-mesh susceptors subjected to a magnetic field is the resulting nonuniform temperature distributions. Induction coils typically generate nonuniform magnetic fields, though uniform fields can be generated for a few specific coil designs with limited work areas (center of a circular coil). Nonuniform fields result in temperature gradients exceeding the processing window required for composite heating or bonding. The focus of this work is on developing a new technique using a metal mesh with specifically designed cut patterns to generate uniform temperature distributions for nonuniform magnetic fields generated by the coil. The presence of cut patterns in a mesh alters the flow of induced eddy currents and, the cut pattern can be optimized to generate uniform temperature distributions.

Mesh density is also an important parameter. If the mesh is too coarse [4], in-plane temperature gradients between two mesh segments can be large. On the other hand, if the mesh is too fine [4], there can be poor resin flow across the mesh, resulting in poor bond strengths. Another common problem is the lack of resin material available for flow and bonding during healing and consolidation. Embedding the mesh in the appropriate polymer system mitigates this problem.

This paper describes a heat-generation model, based on a resistive network-type approach, to predict heat generation in a mesh with cut patterns. Results for several simple cut patterns that show significant improvements in the uniformity of the heat-generation patterns in the mesh susceptor are presented. Experimental tests were performed by inductively heating coarse aluminum meshes, with and without cut patterns. A 1-kW Ameritherm induction heater, with a 3.75-cm-diameter circular coil, was used for this purpose. Temperatures in the mesh were measured using infrared thermography. Qualitative comparisons of heat-generation patterns and measured temperature distributions are presented.

2. Induction-Heating Process

In a typical induction-bonding process, the susceptor (or heating element) is placed between two composite adherends to generate heat at the bondline. In order to have adequate resin flow and consolidation, the susceptor typically contains some resin, such as in resin-impregnated metal meshes, or an extra layer of resin can be added at the bondline. Consolidation pressure is generally applied by vacuum-bagging, though nonmetallic rollers may be used for additional pressure. The induction coil used is designed to "fit" the part, which is one of the major advantages of induction heating. The coil can be designed to fit complex part shapes and geometries. For large parts, the coil can be moved at a specified velocity to provide necessary heating.

The two key requirements of the susceptor are: (1) uniform temperature distribution in the susceptor layer and (2) temperature control to avoid thermal degradation of the susceptor, resin

at the bondline or the composite substrate. It is important to note that the use of "uniform temperature distribution" does not necessarily imply the equal heat generation throughout the susceptor. Instead, the focus is on maintaining the temperature within the processing window of the composite. Temperature gradients may occur within the susceptor and still remain within the processing window. Based on bonding models [11–13] for thermoplastics, this is a key requirement to ensure uniform quality and bond strength.

For the metal-mesh susceptor, uniform temperature distribution can be achieved by the presence of cut patterns in the susceptor to redirect current flow paths. The cut patterns will also alter the heat-generation and heat-transfer mechanisms and an optimized cut pattern can be developed based on a combined heat-generation and heat-transfer model. Bondline temperature control can be achieved by feedback control based on temperature measurements by infrared thermometry or thermocouples of the input power to the system and by coil-susceptor design. The present effort focuses on modeling heat generation in a susceptor due to cuts in the mesh and experimental validation. Results for the combined heat-generation and heat-transfer model, cut pattern optimization, and bondline control will be published at a later date

Predicting heat generation in a metal-mesh susceptor with cut patterns involves two main steps: (1) calculating the magnetic field generated by the induction coil and (2) calculating the heat generated due to the eddy currents in the mesh susceptor.

3. Induction Coil

Magnetic field generated by the coil was calculated based on fundamental electromagnetic principles. The general formula for the magnetic field intensity H, at some point P, due to an electrical current I in an element of conductor (Figure 1) is given by

$$dH = \frac{I}{4\pi} \frac{\vec{dl} \times \vec{r}}{|r|^3} \quad [A/m], \tag{1}$$

where $\vec{dl}$ is an element of the current-carrying conductor and $\vec{r}$ is the position vector between the element $\vec{dl}$ and the point P. By integrating over the whole length of the conductor (the coil in this case), the magnetic field intensity H can be obtained at P, due to the entire induction coil of length L, as

$$H = \frac{I}{4\pi} \int_0^L \frac{\vec{dl} \times \vec{r}}{|r|^3} \quad [A/m] \tag{2}$$

The integral can become complicated depending on the coil shape necessitating the use of numerical techniques to evaluate the intensity at each point. The field was calculated over a 40×40 grid on a surface (the area to be heated), which is some known distance from the coil. This is typically the case in an induction-heating application, where the work piece is placed at a specified distance from the coil.

Figure 2 shows three commonly used coils and the Z component, H_Z, of the generated magnetic field. Only the Z component of the generated field is of interest because it is the component normal to the surface of the mesh susceptor and causes heating. The circular coil pattern for generating uniform temperatures in the susceptor. However, circular coils are best suited for cases where the part to be bonded can be placed inside the coil, which, in general, represents a severe geometric constraint. Pancake and conical coils are the more commonly used "one-sided" coils, and they generate nonuniform fields.

The spacing between the induction coil and the susceptor affects the magnetic field in the plane of the susceptor. Figure 3 shows the effect of increasing coil-susceptor spacing. H_Z is the field intensity at the center of the coil, and H_{Zmax} is the intensity at the same point for a separation distance of 0.1 mm, which was assumed to be the closest possible location of susceptor. The magnetic field drops exponentially with distance from the coil, as expected from equation (2), resulting in a similar reduction in the heat generated by the susceptor. However, metal-mesh susceptors require much smaller amounts of magnetic energy for heating compared

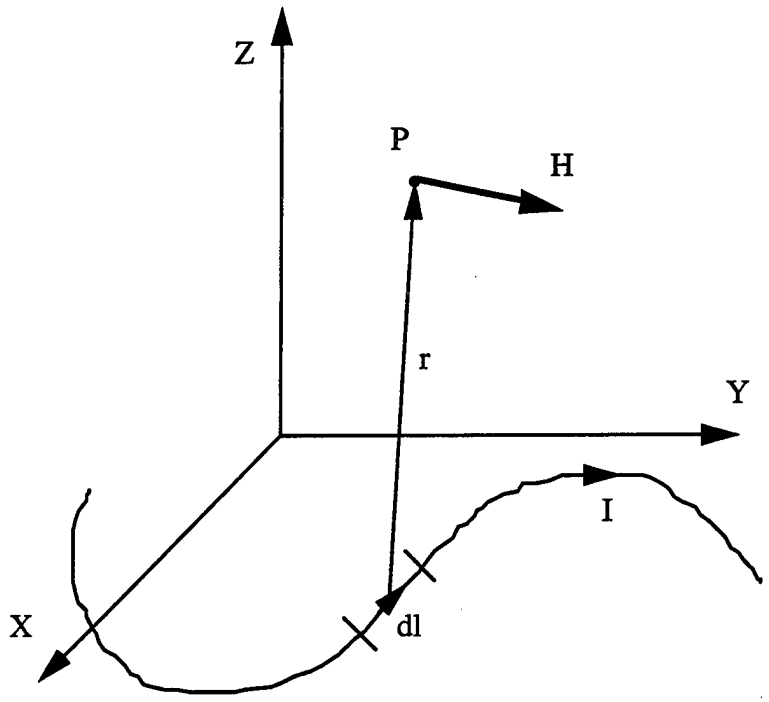

Figure 1. Calculation of Magnetic Field Due to a Current-Carrying Conductor.

to bulk materials and, in some cases, the distance problem can be overcome by increasing the input power to the coil. One can also increase the frequency of the current in the induction coil. Typical metallic heating applications use kilohertz range frequencies, which may be increased up to several megahertz when higher heating rates are required.

4. Cut-Mesh Concept

In metal-mesh susceptors, heat is generated in each mesh segment due to eddy currents induced by an alternating magnetic field. The uniformity of current generated in the mesh depends on both the coil and the mesh configuration. It is a well-known problem that, for general or commonly used induction coils, the generated fields are nonuniform, resulting in nonuniform heat generation and significant temperature gradients over the mesh area. Experiments conducted with coarse aluminum meshes showed gradients of over 80°C in a 6.25-cm × 6.25-cm mesh.

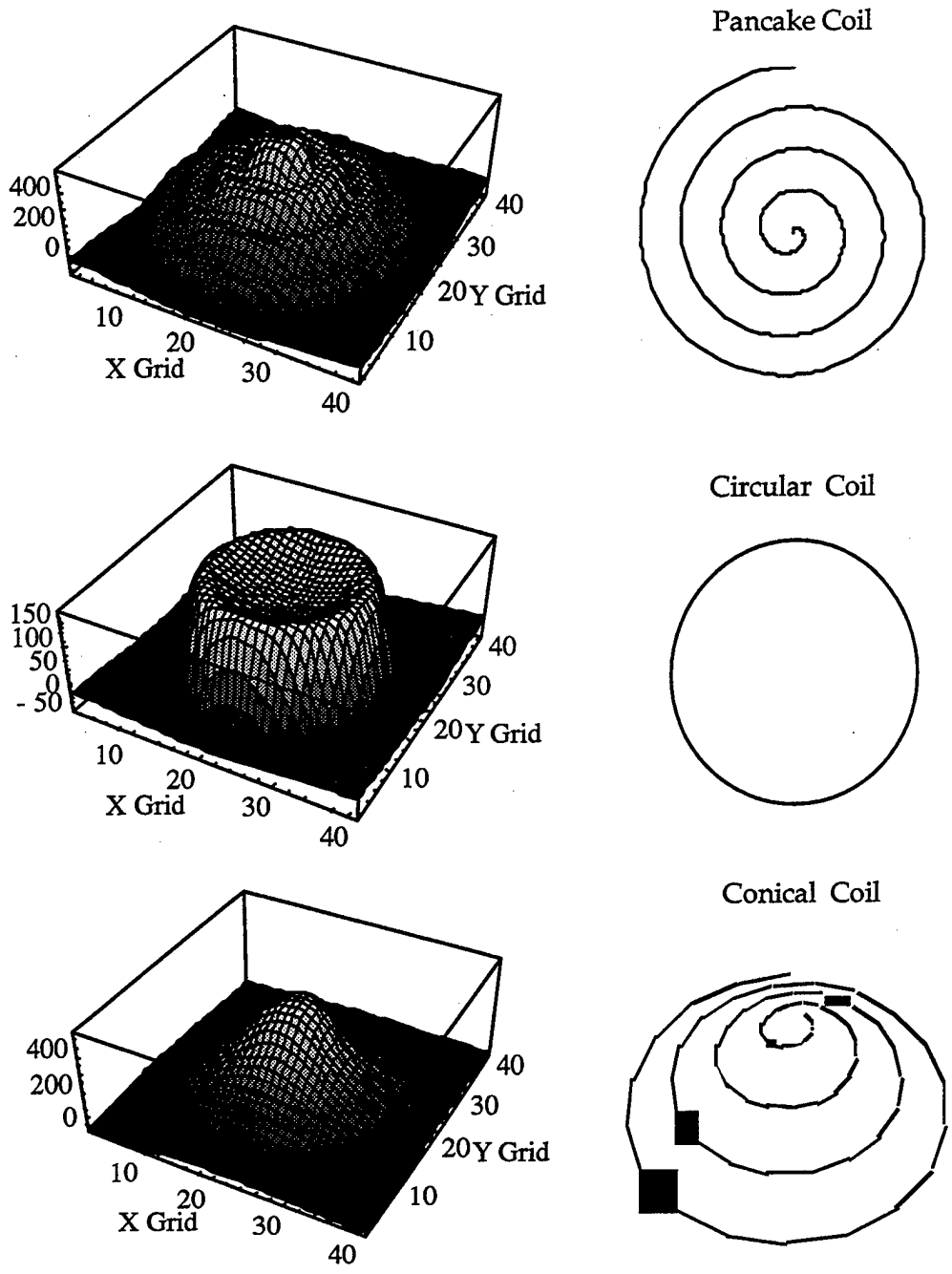

Figure 2. Typical Magnetic Fields (Z Component) Generated by Induction Coils on a 40 × 40 Grid Surface Located 1 cm From Coil. Units Are $-4\pi H_z/I$.

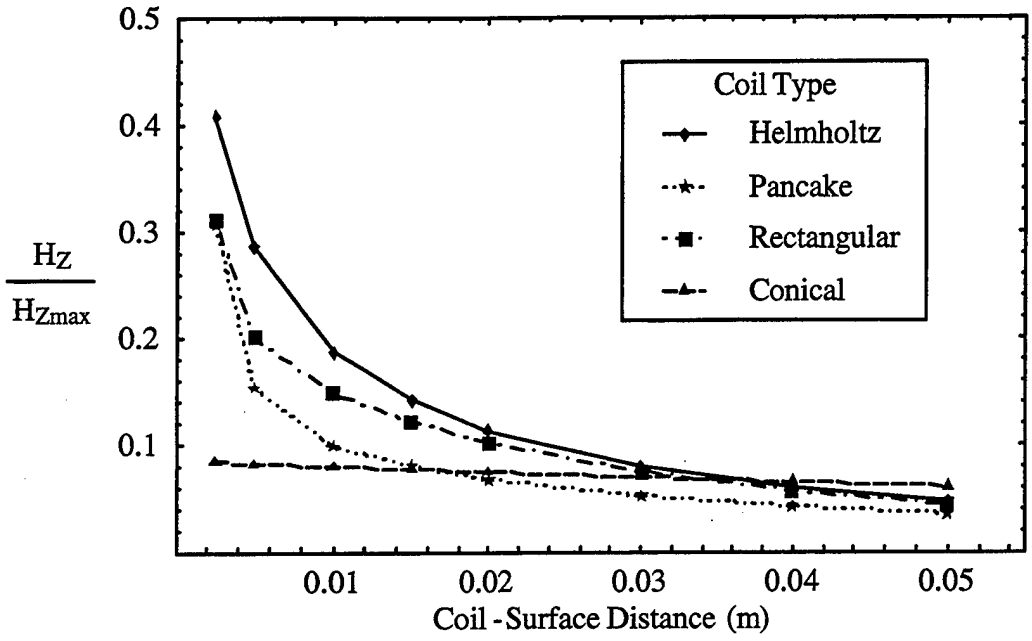

Figure 3. Effect of Coil-Susceptor Distance on the Magnetic Field at the Susceptor.

If a region of the mesh is considered, where the heat generation is the highest, removing one or more mesh segments will alter the induced currents. By selective removal of segments of the mesh, one can alter the induced current pattern such that the resultant heating patterns and temperature distributions are more uniform and within the desired processing window. This leads to the following design concept.

Uniform temperature in a metal-mesh susceptor, subject to nonuniform magnetic fields, may be achieved by specifically designed cut patterns, based on the induction coil and mesh used. Mesh optimization is required to identify the best possible cut pattern.

5. Heat-Generation Model

5.1 Uniform-Mesh Calculations. The alternating magnetic field generated by the induction coil induces eddy currents in the mesh susceptor, and the resistance of the mesh material

produces heat. The induced electromotive force (emf), in a closed loop in the mesh, can be calculated from:

$$\text{emf} = 2\pi f \mu_o \int_S \mathbf{H} \cdot \vec{n}\, dA = 2\pi f \mu_o \sum_{i=1}^{m} \sum_{j=1}^{n} H_{z_{ij}} dA, \tag{3}$$

where, f is the current frequency, μ_o is permittivity in free space, $\vec{n}$ is a unit vector normal to the mesh surface, and H_Z is the Z component of the magnetic field at the surface of the mesh. The double summation is used instead of the area integral, because of the field being calculated numerically, over an m × n grid (Figure 4). For example, if a 10 × 10 square mesh was used and the field calculated over a 40 × 40 grid, each mesh box would have a 4 × 4 grid of magnetic field values to calculate the emf.

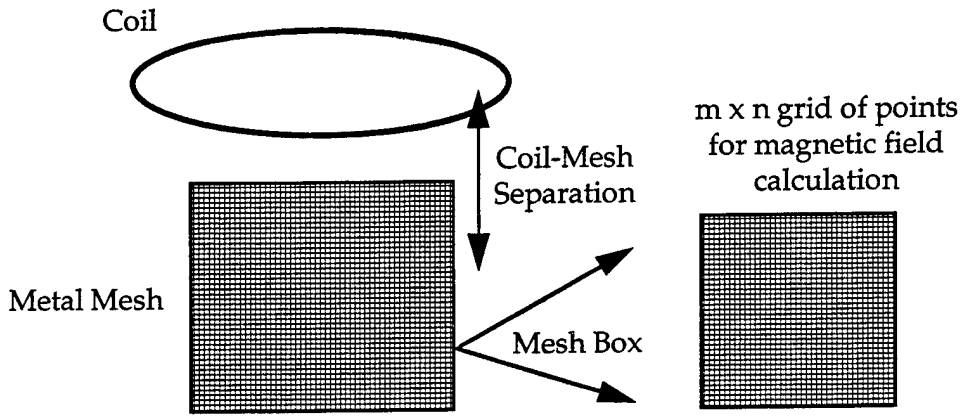

Figure 4. Schematic of Coil and Mesh Configuration.

Since the mesh has a number of closed loops and different loop shapes (in the case of cut patterns), a resistor network-type calculation was used to determine the emf's in each segment of the mesh. Each segment of the mesh was assumed to carry an unknown voltage or current. Current conservation laws were applied at each mesh box corner or node and along with the emf equations for each closed loop (induced emf equals the sum of voltages in the loop), and a set of linear algebraic equations was obtained, which is solved for the unknown currents. Knowing the

resistance of each segment (from wire geometry and material resistivity), the heat generated in each segment of a mesh box can be calculated. The following simple example of a 2×2 mesh illustrates the procedure.

For the 2×2 mesh shown in Figure 5, with each mesh segment having resistance R, the induced emf and current conservation equations are as follows.

Induced emf:

$$\begin{aligned} I_1 + I_2 + I_3 + I_4 &= emf_1/R, \\ -I_3 + I_5 + I_6 + I_7 &= emf_2/R, \\ -I_4 + I_8 + I_9 + I_{10} &= emf_3/R, \text{ and} \\ -I_9 - I_7 + I_{11} + I_{12} &= emf_4/R. \end{aligned} \tag{4a}$$

Current conservation at nodes:

$$\begin{aligned} I_1 = I_2,\ I_5 = I_6,\ I_{11} = I_{12},\ I_8 = I_{10}, \\ I_2 = I_3 + I_5, \\ I_6 = I_7 + I_{11}, \\ I_9 + I_{12} = I_{10}, \\ I_8 + I_4 = I_1, \text{ and} \\ I_3 + I_7 = I_4 + I_9. \end{aligned} \tag{4b}$$

The resulting system of 12 unknown currents and 13 equations is solved to calculate currents induced in the mesh segments. Because the system of equations is linear, solving large systems for fine or high-density meshes is not a significant computational exercise and can be done in a relatively short time. Symmetry of field and mesh can also be used to reduce computational time.

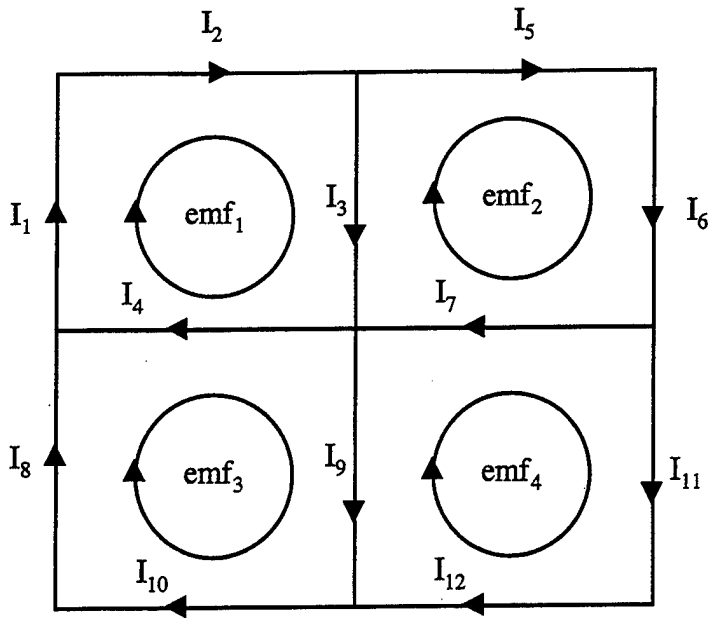

Figure 5. Schematic of Induced Currents in a 2 × 2 Mesh.

5.2 Cut-Mesh Calculations. To generate uniform temperature distributions within the mesh susceptor, segments of the meshes can be cut to redirect current flow within the mesh. Based on the applied field distribution, preferential heating will occur and cutting segments will force changes in the path of current flow in the mesh and can equalize heating to some extent. The current calculation technique outlined previously can be easily adapted for a cut-mesh case.

Consider the same 2 × 2 mesh in Figure 5 with one of the segments cut, as shown in Figure 6. The induced emf and current conservation equations are as follows.

Induced emf:

$$I_1 + I_2 + I_3 + I_4 = emf_1/R,$$
$$-I_3 + I_5 + I_6 + I_7 = emf_2/R, \text{ and}$$
$$-I_4 - I_7 + I_8 + I_9 + I_{10} = emf_3/R. \qquad (5a)$$

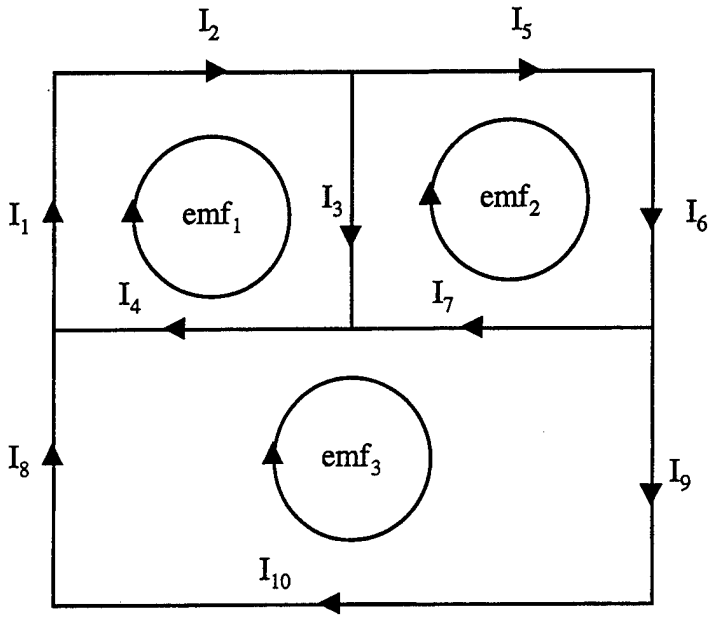

Figure 6. Schematic of Induced Currents in a 2 × 2 Mesh With a Cut Segment.

Current conservation at nodes:

$$I_1 = I_2\ ,\ I_5 = I_6\ ,\ I_8 = I_{10}\ ,\ I_9 = I_{10},$$
$$I_2 = I_3 + I_5,$$
$$I_8 + I_4 = I_1,$$
$$I_6 = I_7 + I_9, \text{ and}$$
$$I_3 + I_7 = I_4. \qquad (5b)$$

Comparing these equations with the uncut case, the induced emfs are different. Cutting one of the segments forces a "redirection" of the current loops, resulting in significantly different heat generation in each mesh segment. Larger meshes with more complicated cut patterns can be easily handled by this model. A computer program was developed for this purpose. Some heat-generation predictions for different cut patterns are presented in the results.

The model outlined previously can successfully handle any cutout configuration in the mesh and predict the appropriate induced currents and voltages. Meshes of up to 40 × 40, with many

different cut patterns, were solved by this model. While the algorithm predicts heat generation, experimental verification requires estimating temperature as the mesh heats up, since temperature is the measured quantity. However, because induction heating is a rapid heating process, especially in metals, one can qualitatively compare measured temperature patterns to the predicted heat-generation patterns at short times. Integrating the mesh model with a heat-transfer model will allow actual temperature comparisons.

One effect that can be neglected is the opposing field that is generated by the induced currents in the mesh wires, also known as "back emf." This field will oppose the applied magnetic field, as a result of which, the actual field is smaller. For sparse meshes, the opposing field effect will be small; however, if fine meshes are used, it may no longer be possible to neglect this effect. This effect was quantified by experiments where the frequency of the alternating current in the coil was noted with and without the mesh susceptor. If the inverse field effect is significant, a change in frequency is expected, with larger changes in frequency for larger inverse fields. For all the meshes studied, ranging from coarse 4×4 to finer 120×120 per square inch mesh density, there was no significant change in frequency ($f = 275$ kHz, $\Delta f <$ 1 kHz), which implies a negligible back emf effect due to the mesh. Due to the negligible effect, the induction system can be designed to operate at any desired frequency. This effect is more prevalent in the case of bulk heating.

6. Results

The mesh model was used to predict heat generation in meshes with or without cut configurations. For the purposes of qualitative comparison with experimental temperature measurements, heat-generation values along the X- and Y-axis of the mesh were calculated. In all the modeling results presented, change in resistance of the mesh material was not considered, since the model only predicted heat generation and not temperatures.

A schematic of the experimental setup is shown in Figure 7. The induction system used was a water-cooled 1-kW Ameritherm system, with a frequency range from 50 to 450 kHz. The induction coil was fabricated from copper tubing, 0.125-in to 0.25-in outer diameter, to facilitate water cooling during operation. The coil shape, size, and geometry are design parameters and for the results presented, a 3.75-cm-diameter circular coil was used. The meshes used were coarse aluminum meshes with a mesh density of 4×4 per square inch and manufactured by Unique Wire Weaving Company. The meshes were not impregnated with any material, since there is no heat-transfer component in the mesh model to account for thermal conductivity of the material. Temperature measurements were made using an AGEMA Thermovision 900 infrared (IR) system, which permitted far-field noncontact temperature measurements in the meshes. During heating tests, both the coil and the mesh were suspended in air and at a constant separation distance of 1 cm.

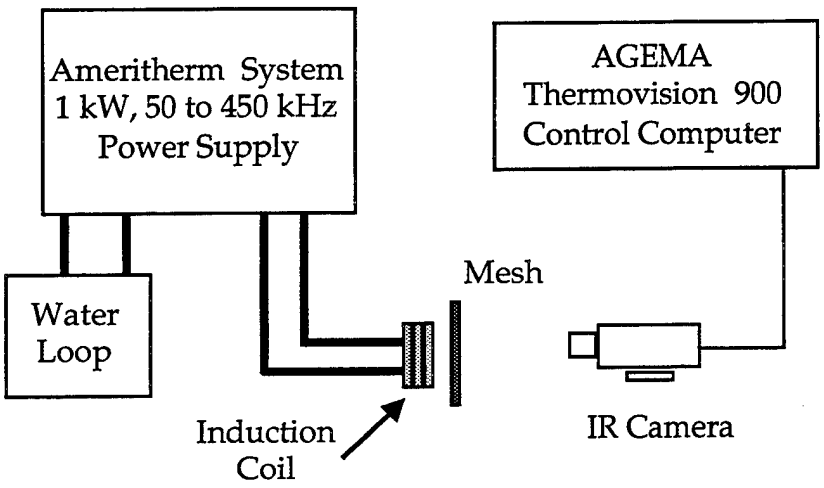

Figure 7. Schematic of Induction-Heating Setup.

6.1 Heat-Generation Model Predictions. Figure 8 shows typical heat-generation profiles for an uncut mesh for the four-turn pancake coil whose field is shown in Figure 2. The two curves show the profiles at the midlines of a 10×10 square (6.25×6.25 cm) aluminum mesh, in the X and Y directions. As expected, the heat-generation profiles are nonuniform, which is the

main drawback to using nonoptimal coil/mesh susceptor combinations. A mesh gradient factor (MGF), defined as

$$\mathrm{MGF} = \frac{\text{Maximum Heat Generation}}{\text{Minimum Heat Generation}}, \tag{6}$$

is used as a quality factor. For the heat-generation profile in Figure 8, this factor is approximately 4.7, which implies a large temperature gradient along either axis.

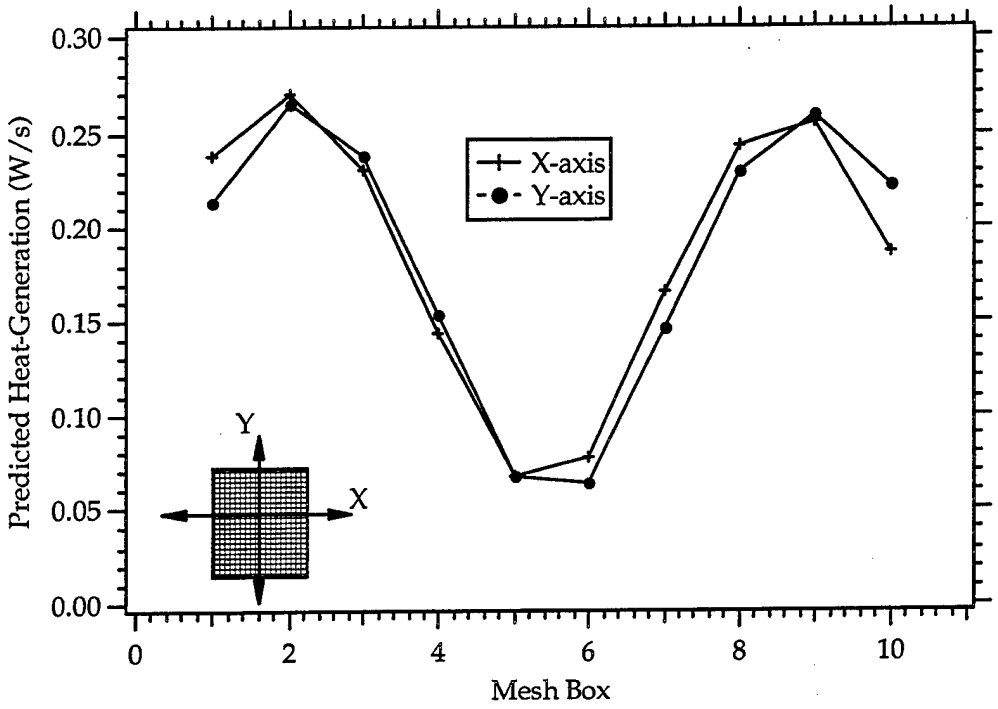

Figure 8. Heat-Generation Profile for a 10 × 10 Square Uncut Aluminum Mesh: Pancake Coil.

The response of three different cut patterns (Figure 9) to the four-turn pancake coil investigated are shown in Figures 10 and 11 with comparison to the uncut case. As expected, the uncut case shows the highest heat-generation differential along either the X or Y direction. The cut locations were chosen at points where the heat generation was maximum for the uncut case and for few cuts, a significant drop in the heat-generation gradient can be seen.

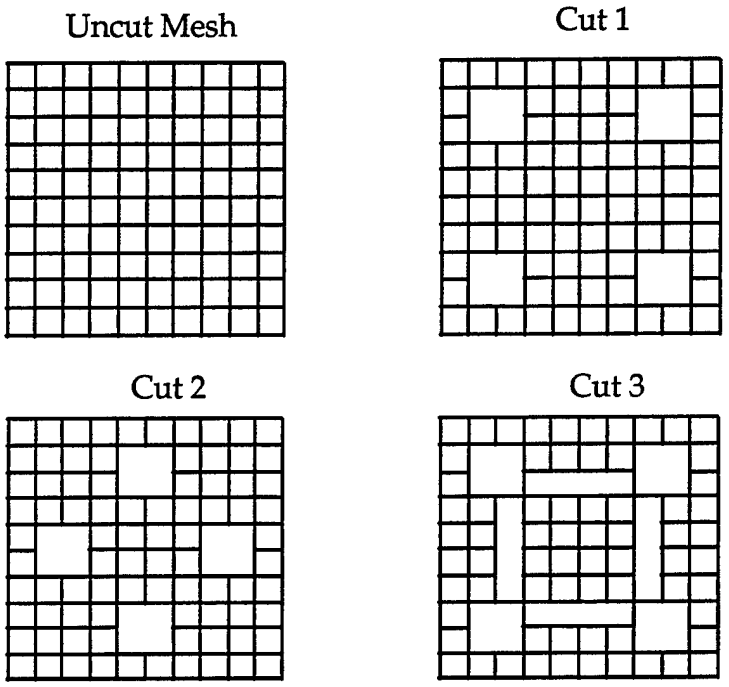

Figure 9. Mesh Configurations for Cut/Uncut Case Studies.

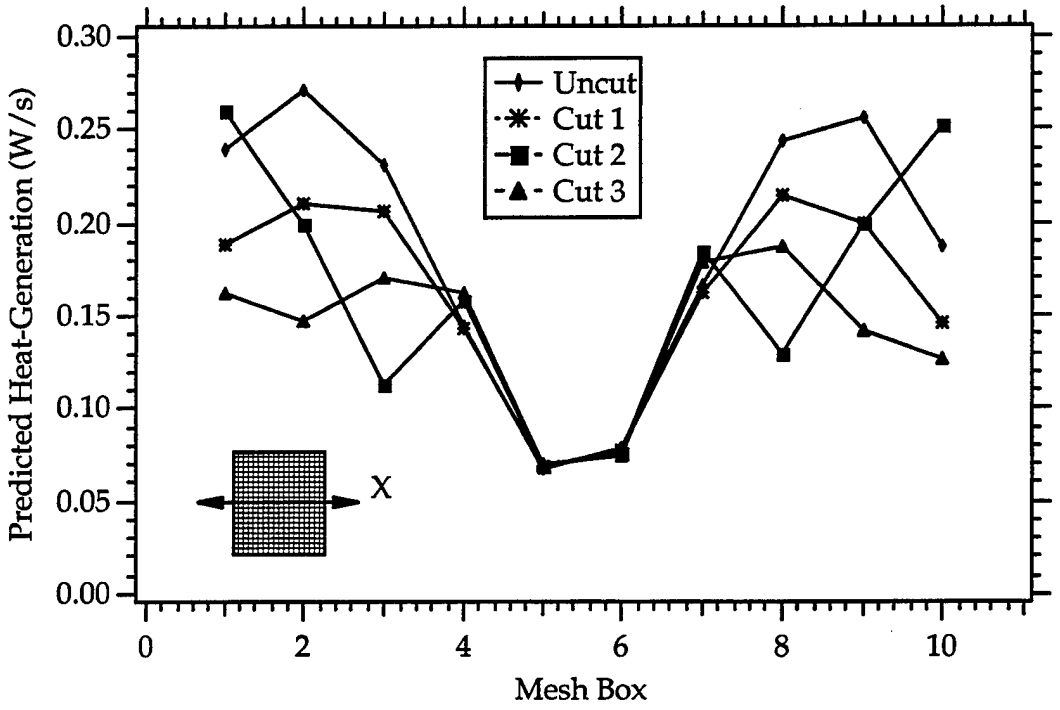

Figure 10. X-Axis Heat Generation for a 10 × 10 Square Aluminum Mesh: Pancake Coil.

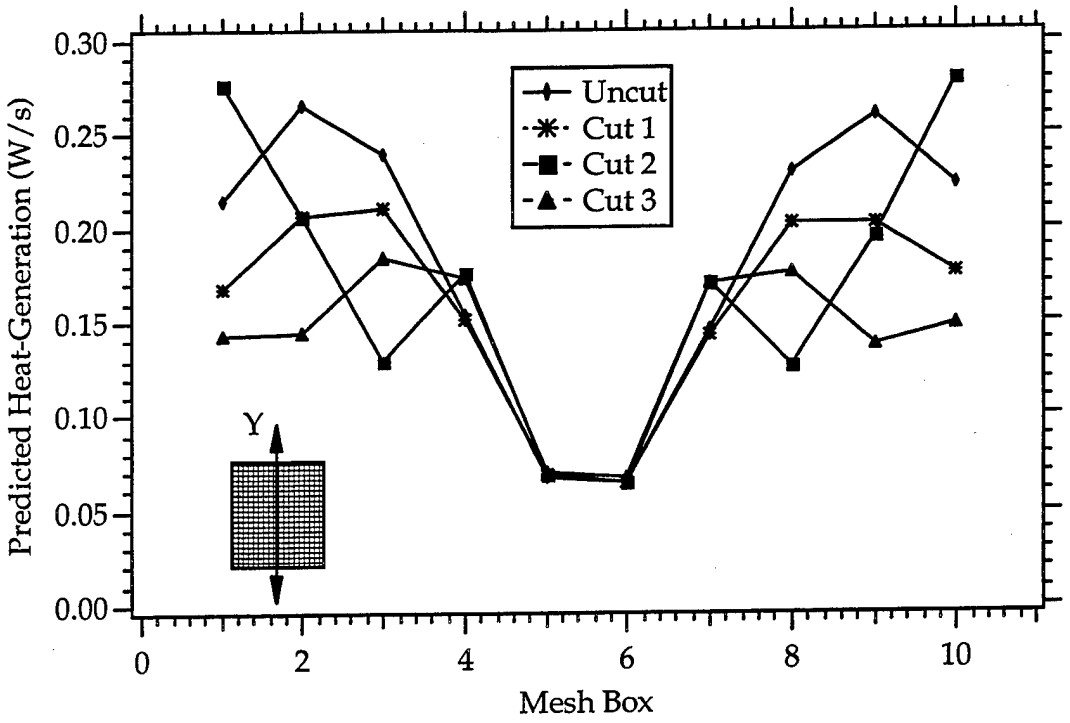

Figure 11. Y-Axis Heat Generation for a 10 × 10 Square Aluminum Mesh: Pancake Coil.

The MGFs in the three cut cases are 4.5, 3.6, and 2.9, respectively, which compares favorably to the uncut baseline (4.7). The lower the ratio, the more uniform the temperature distribution will be. While it is expected that impregnation of the mesh with polymer will reduce the gradient somewhat, due to conduction in the polymer, the reduction will be small. This is because of the high heating rates in the mesh. One can further optimize the cutting pattern to identify the best pattern in terms of the final temperature distribution. This can be done by combining the heat-generation model with an unsteady-state heat-transfer model to predict temperature patterns. Finer meshes will also allow better control of the temperature distribution.

6.2 Experimental Results. Experiments were conducted with coarse aluminum meshes to measure temperature distributions in the mesh during heating. Figure 12 shows the results for an uncut-mesh case, with measured temperature profiles and predicted heat generation along the X-axis and the Y-axis. The temperature profiles follow the predicted heat-generation patterns very well and this serves as a good qualitative check for the model. Actual temperature comparisons will be made after combining the heat-generation model with an unsteady-state heat-transfer model.

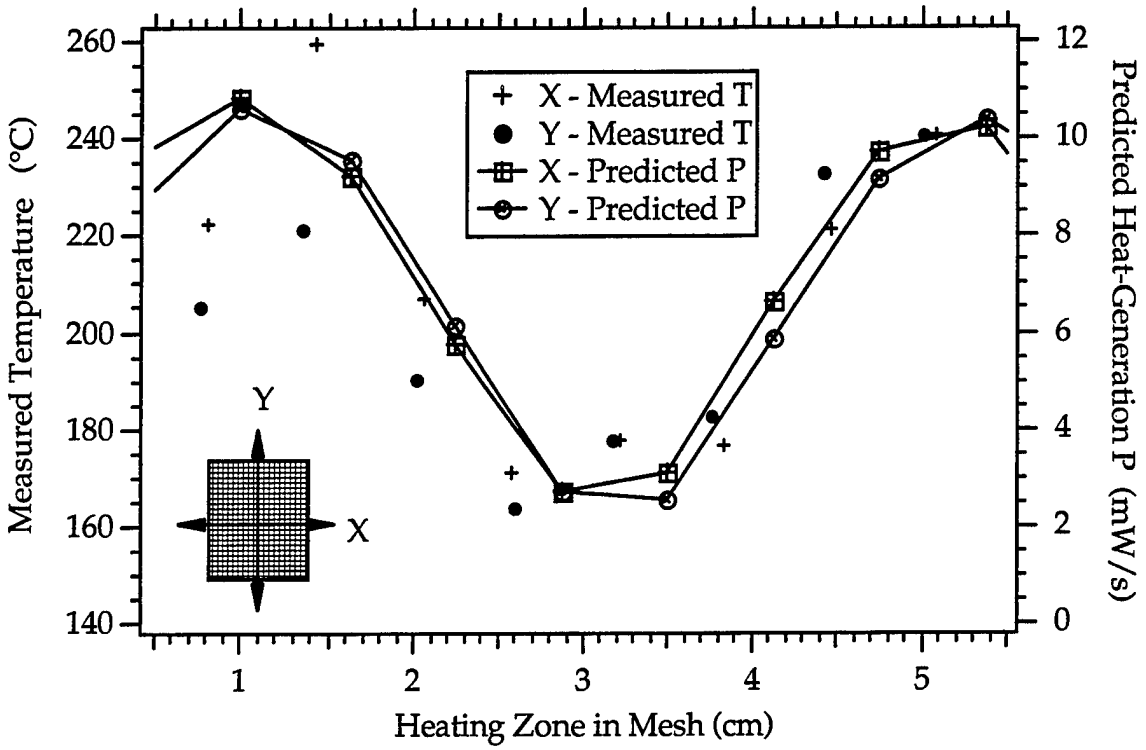

Figure 12. Temperature Profiles for Uncut Mesh viz. Predicted Heat Generation.

Figure 12 shows a heating zone in the mesh, which is the area of the mesh that will show "uniform temperature distribution." Generally, the heating zone in the mesh is approximately the same as the coil area. Outside this zone, temperatures will be much smaller because of the rapid decay in magnetic field. Heating zones become important when coil motion is considered for large composite parts.

The temperature differential between the maximum and the minimum points on the mesh is approximately 80°C (180 to 260°C). This is not an acceptable range, as typical processing windows are much smaller (e.g., $\Delta T = \pm 20°C$). A designed cut pattern can be used to reduce the temperature differential, and an example is shown in Figure 13. In this example, the Y-axis temperatures are shown, comparing the measured temperatures for the uncut case in Figure 12 with the cut case. The mesh patterns (uncut and cut) are shown in Figure 14. Cuts were made along segments showing high temperatures, since temperature patterns follow heat-generation patterns and the temperature differential drops from 80°C to 40°C. There is also a drop in

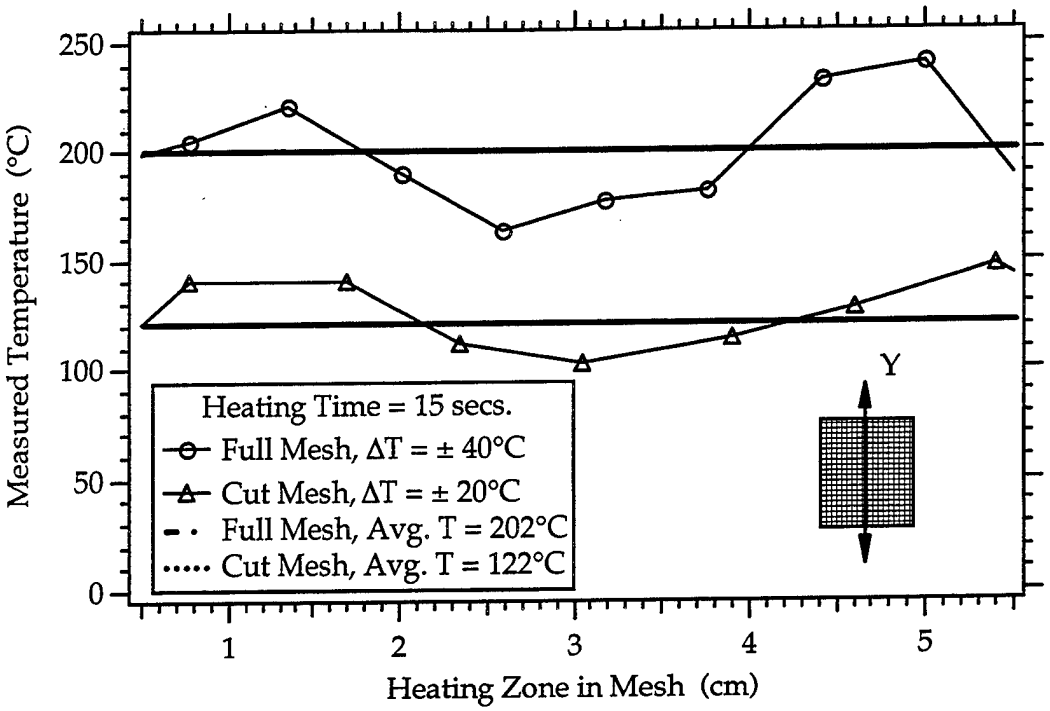

Figure 13. Effect of Cut Pattern on Temperature Distribution in Mesh: Constant Time.

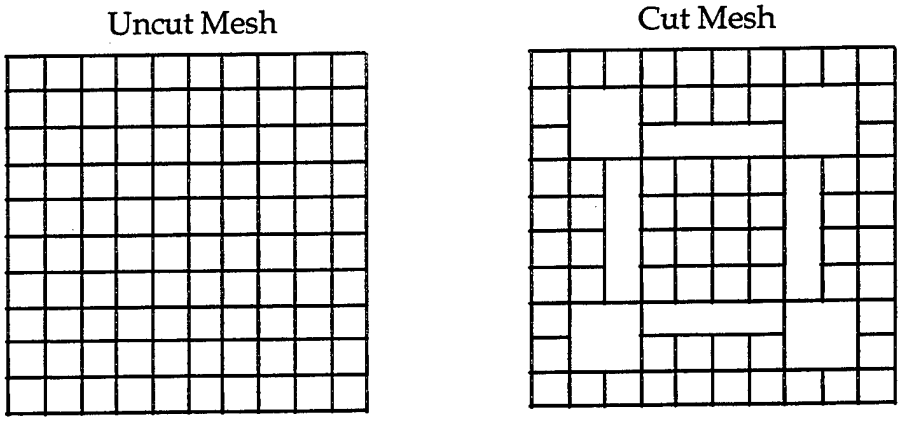

Figure 14. Mesh Patterns for Temperature Measurements.

temperature for the same heating time (15 s), which can be rectified by heating for a longer period or increasing power (Figure 15). Increasing power or heating time did not change the temperature differential for a specific mesh configuration. Further optimization of mesh patterns (based on heat-generation/heat-transfer model) is necessary to further reduce the temperature differential within ±20°C.

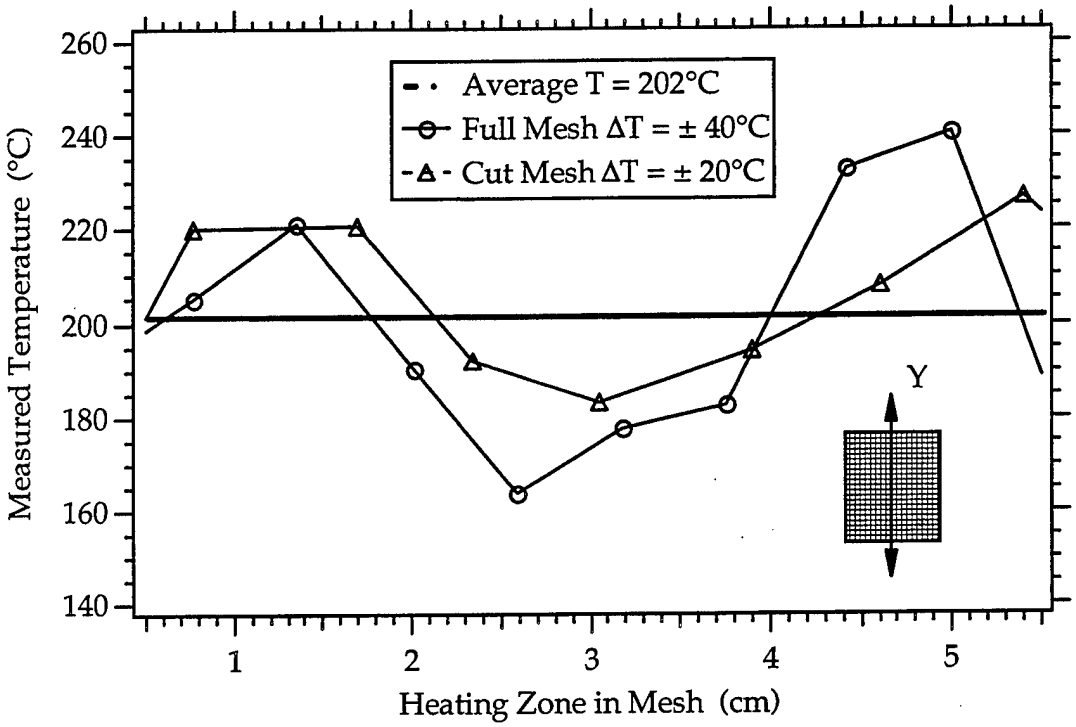

Figure 15. Effect of Cut Pattern on Temperature Distribution in Mesh: Constant Average Temperature.

7. Conclusions

A new concept for resistive-mesh susceptors, based on specifically designed cuts to obtain uniform temperature distributions in the bondline during induction bonding, was investigated. A resistor network-based model was developed to predict heat generation in a metal mesh for cut patterns of any size and shape. Theoretical and experimental results demonstrate that significantly reduced thermal gradients are possible using designed cut patterns. Qualitative comparisons of heat-generation predictions using the mesh model and measured temperatures of induction heated meshes agree very well.

In order to use mesh susceptors for composite bonding, temperature predictions at the bondline (in the mesh) are critical, as bonding performance is directly influenced by temperature. The mesh model presented in this work is a first step toward developing a mesh-susceptor-based integrated bonding model. Future work will focus on combining the model with heat-transfer and bond-strength prediction models.

INTENTIONALLY LEFT BLANK.

8. References

1. Don R. C., S. H. McKnight, and J. W. Gillespie, Jr. "Bonding Techniques for High-Performance Thermoplastic Compositions." U.S. Patent No. 5,643,390, 1997.

2. Weider, S. M., H. J. Lause, and R. Fountain. "Structural Repair Systems for Thermoplastic Composites." *Composite Repairs: SAMPE Monograph No. 1*, edited by Brown, SAMPE, Covina, CA, 1985.

3. Benatar, A., and T. G. Gutowski. "Methods for Fusion Bonding Thermoplastic Composites." *SAMPE Quarterly*, October 1986.

4. Border, J., and R. Salas. "Induction Heated Joining of Thermoplastic Composites Without Metal Susceptors." *34th SAMPE Symposium*, 1989.

5. Nagumo, T., H. Makamura, Y. Yoshida, and K. Hiraoka. "Evaluation of PEEK Matrix Composites." *32nd International Symposium, SAMPE*, 1987.

6. Buckley, J. D., R. L. Fox, and J. R. Tyeryar. "Seam Bonding of Graphite Reinforced Composite Panels." NASA Advanced Composites Conference, 1986.

7. Lewis, C. F. "Materials Keep a Low Profile." *Materials Engineering*, vol.105, 1988.

8. Buckley, J. D., and R. L. Fox. "Rapid Electromagnetic Induction Bonding of Composites, Plastics and Metals." Materials Research Society Symposium, vol. 124, 1988.

9. Lawless, G. W., and T. J. Reinhart. "Study of the Induction Heating of Organic Composites." *International SAMPE Conference*, Toronto, Canada, October 1992.

10. Wedgewood, A. R., and P. E. Hardy. "Induction Welding of Thermoset Composite Adherends Using Thermoplastic Interlayers and Susceptors." *International SAMPE Conference*, vol. 28, Seattle, WA, November 1996.

11. Butler, C. A., R. L. McCullough, and A. R. Wedgewood. "Interaction Between Healing and Intimate Contact During Fusion Bonding of Thermoplastic Composite Materials." *Proceedings of the American Institute of Chemical Engineers*, AICHE Annual Meeting, 1994.

12. Butler, C. A., R. Pitcliumani, R. L. McCullough, and A. R. Wedgewood. "Coupled Effects of Healing and Intimate Contact During Thermoplastic Fusion Bonding." *Proceedings of the 10th Annual ASM/ESD Advanced Composites Conference,* pp. 595–604, 1994.

13. Tierney, J. J., R. F. Eduljee, and J. W. Gillespie, Jr. "Material Response During Robotic Tow Placement of Thermoplastic Composites." *Proceedings of the 11th Annual Advanced Composites Conference,* pp. 315–329, November 1995.

NO. OF COPIES ORGANIZATION

2 DEFENSE TECHNICAL INFORMATION CENTER
DTIC DDA
8725 JOHN J KINGMAN RD
STE 0944
FT BELVOIR VA 22060-6218

1 HQDA
DAMO FDQ
D SCHMIDT
400 ARMY PENTAGON
WASHINGTON DC 20310-0460

1 OSD
OUSD(A&T)/ODDDR&E(R)
R J TREW
THE PENTAGON
WASHINGTON DC 20301-7100

1 DPTY CG FOR RDA
US ARMY MATERIEL CMD
AMCRDA
5001 EISENHOWER AVE
ALEXANDRIA VA 22333-0001

1 INST FOR ADVNCD TCHNLGY
THE UNIV OF TEXAS AT AUSTIN
PO BOX 202797
AUSTIN TX 78720-2797

1 DARPA
B KASPAR
3701 N FAIRFAX DR
ARLINGTON VA 22203-1714

1 NAVAL SURFACE WARFARE CTR
CODE B07 J PENNELLA
17320 DAHLGREN RD
BLDG 1470 RM 1101
DAHLGREN VA 22448-5100

1 US MILITARY ACADEMY
MATH SCI CTR OF EXCELLENCE
DEPT OF MATHEMATICAL SCI
MADN MATH
THAYER HALL
WEST POINT NY 10996-1786

NO. OF COPIES ORGANIZATION

1 DIRECTOR
US ARMY RESEARCH LAB
AMSRL DD
2800 POWDER MILL RD
ADELPHI MD 20783-1197

1 DIRECTOR
US ARMY RESEARCH LAB
AMSRL CS AS (RECORDS MGMT)
2800 POWDER MILL RD
ADELPHI MD 20783-1145

3 DIRECTOR
US ARMY RESEARCH LAB
AMSRL CI LL
2800 POWDER MILL RD
ADELPHI MD 20783-1145

ABERDEEN PROVING GROUND

4 DIR USARL
AMSRL CI LP (BLDG 305)

NO. OF
COPIES ORGANIZATION

1 DIRECTOR
USARL
AMSRL CP CA D SNIDER
2800 POWDER MILL RD
ADELPHI MD 20783

1 COMMANDER
USA ARDEC
AMSTA AR FSE T GORA
PICATINNY ARSENAL NJ
07806-5000

3 COMMANDER
USA ARDEC
AMSTA AR TD
PICATINY ARSENAL NJ
078806-5000

5 COMMANDER
USA TACOM
AMSTA JSK
S GOODMAN
J FLORENCE
AMSTA TR D
B RAJU
L HINOJOSA
D OSTBERG
WARREN MI 48397-5000

5 PM SADARM
SFAE GCSS SD
COL B ELLIS
M DEVINE
W DEMASSI
J PRITCHARD
S HROWNAK
PICATINNY ARSENAL NJ
07806-5000

1 COMMANDER
USA ARDEC
F MCLAUGHLIN
PICATINNY ARSENAL NJ
07806-5000

NO. OF
COPIES ORGANIZATION

5 COMMANDER
USA ARDEC
AMSTA AR CCH
S MUSALLI
R CARR
M LUCIANO
T LOUCEIRO
PICATINNY ARSENAL NJ
07806-5000

4 COMMANDER
USA ARDEC
AMSTA AR (2 CPS)
E FENNELL (2 CPS)
PICATINNY ARSENAL NJ
07806-5000

1 COMMANDER
USA ARDEC
AMSTA AR CCH P J LUTZ
PICATINNY ARSENAL NJ
07806-5000

1 COMMANDER
USA ARDEC
AMSTA AR FSF T C LIVECCHIA
PICATINNY ARSENAL NJ
07806-5000

1 COMMANDER
USA ARDEC
AMSTA AR QAC T/C C PATEL
PICATINNY ARSENAL NJ
07806-5000

2 COMMANDER
USA ARDEC
AMSTA AR M
D DEMELLA
F DIORIO
PICATINNY ARSENAL NJ
07806-5000

NO. OF
COPIES ORGANIZATION

3 COMMANDER
USA ARDEC
AMSTA AR FSA
A WARNASH
B MACHAK
M CHIEFA
PICATINNY ARSENAL NJ
07806-5000

1 COMMANDER
SMCWV QAE Q
B VANINA
BLDG 44 WATERVLIET ARSENAL
WATERVLIET NY 12189-4050

1 COMMANDER
SMCWV SPM
T MCCLOSKEY
BLDG 253 WATERVLIET ARSENAL
WATERVLIET NY 12189-4050

8 DIRECTORECTOR
BENET LABORATORIES
AMSTA AR CCB
J KEANE
J BATTAGLIA
J VASILAKIS
G FFIAR
V MONTVORI
G DANDREA
R HASENBEIN
AMSTA AR CCB R
S SOPOK
WATERVLIET NY 12189-4050

1 COMMANDER
SMCWV QA QS K INSCO
WATERVLIET NY 12189-4050

1 COMMANDER
PRODUCTION BASE MODERN
ACTY
USA ARDEC
AMSMC PBM K
PICATINNY ARSENAL NJ
07806-5000

NO. OF
COPIES ORGANIZATION

1 COMMANDER
USA BELVOIR RD&E CTR
STRBE JBC
FT BELVOIR VA 22060-5606

2 COMMANDER
USA ARDEC
AMSTA AR FSB G
M SCHIKSNIS
D CARLUCCI
PICATINNY ARSENAL NJ
07806-5000

1 US ARMY COLD REGIONS
RESEARCH & ENGINEERING CTR
P DUTTA
72 LYME RD
HANVOVER NH 03755

1 DIRECTOR
USARL
AMSRL WT L D WOODBURY
2800 POWDER MILL RD
ADELPHI MD 20783-1145

1 COMMANDER
USA MICOM
AMSMI RD W MCCORKLE
REDSTONE ARSENAL AL
35898-5247

1 COMMANDER
USA MICOM
AMSMI RD ST P DOYLE
REDSTONE ARSENAL AL
35898-5247

1 COMMANDER
USA MICOM
AMSMI RD ST CN T VANDIVER
REDSTONE ARSENAL AL
35898-5247

2 US ARMY RESEARCH OFFICE
A CROWSON
K LOGAN
PO BOX 12211
RESEARCH TRIANGLE PARK NC
27709-2211

NO. OF COPIES ORGANIZATION

3 US ARMY RESEARCH OFFICE
ENGINEERING SCIENCES DIV
R SINGLETON
G ANDERSON
K IYER
PO BOX 12211
RESEARCH TRIANGLE PARK NC
27709-2211

5 PM TMAS
SFAE GSSC TMA
COL PAWLICKI
K KIMKER
E KOPACZ
R ROESER
B DORCY
PICATINNY ARSENAL NJ
07806-5000

1 PM TMAS
SFAE GSSC TMA SMD
R KOWALSKI
PICATINNY ARSENAL NJ
07806-5000

3 PEO FIELD ARTILLERY SYSTEMS
SFAE FAS PM
H GOLDMAN
T MCWILLIAMS
T LINDSAY
PICATINNY ARSENAL NJ
07806-5000

2 PM CRUSADER
G DELCOCO
J SHIELDS
PICATINNY ARSENAL NJ
07806-5000

3 NASA LANGLEY RESEARCH CTR
MS 266
AMSRL VS
W ELBER
F BARTLETT JR
C DAVILA
HAMPTON VA 23681-0001

NO. OF COPIES ORGANIZATION

2 COMMANDER
DARPA
S WAX
2701 N FAIRFAX DR
ARLINGTON VA 22203-1714

6 COMMANDER
WRIGHT PATTERSON AFB
WL FIV
A MAYER
WL MLBM
S DONALDSON
T BENSON-TOLLE
C BROWNING
J MCCOY
F ABRAMS
2941 P ST STE 1
DAYTON OH 45433

2 NAVAL SURFACE WARFARE CTR
DAHLGREN DIV CODE G06
R HUBBARD CODE G 33 C
DAHLGREN VA 22448

1 NAVAL RESEARCH LAB
I WOLOCK CODE 6383
WASHINGTON DC 20375-5000

1 OFFICE OF NAVAL RESEARCH
MECH DIV
Y RAJAPAKSE CODE 1132SM
ARLINGTON VA 22271

1 NAVAL SURFACE WARFARE CTR
CRANE DIV
M JOHNSON CODE 20H4
LOUISVILLE KY 40214-5245

1 DAVID TAYLOR RESEARCH CTR
SHIP STRUCTURES &
PROTECTION DEPT
J CORRADO CODE 1702
BETHESDA MD 20084

2 DAVID TAYLOR RESEARCH CTR
R ROCKWELL
W PHYILLAIER
BETHESDA MD 20054-5000

NO. OF COPIES ORGANIZATION

1 DEFENSE NUCLEAR AGENCY
INNOVATIVE CONCEPTS DIV
R ROHR
6801 TELEGRAPH RD
ALEXANDRIA VA 22310-3398

1 EXPEDITIONARY WARFARE
DIV N85 F SHOUP
2000 NAVY PENTAGON
WASHINGTON DC 20350-2000

1 OFFICE OF NAVAL RESEARCH
D SIEGEL 351
800 N QUINCY ST
ARLINGTON VA 22217-5660

7 NAVAL SURFACE WARFARE CTR
J H FRANCIS CODE G30
D WILSON CODE G32
R D COOPER CODE G32
E ROWE CODE G33
T DURAN CODE G33
L DE SIMONE CODE G33
DAHLGREN VA 22448

1 COMMANDER
NAVAL SEA SYSTEM CMD
P LIESE
2351 JEFFERSON DAVIS HIGHWAY
ARLINGTON VA 22242-5160

1 NAVAL SURFACE WARFARE CTR
M E LACY CODE B02
17320 DAHLGREN RD
DAHLGREN VA 22448

1 NAVAL WARFARE SURFACE CTR
TECH LIBRARY CODE 323
17320 DAHLGREN RD
DAHLGREN VA 22448

4 DIR
LLNL
R CHRISTENSEN
S DETERESA
F MAGMESS
M FINGER
PO BOX 808
LIVERMORE CA 94550

NO. OF COPIES ORGANIZATION

2 DIRECTOR
LLNL
F ADDESSIO MS B216
J REPPA MS F668
PO BOX 1633
LOS ALAMOS NM 87545

3 UNITED DEFENSE LP
4800 EAST RIVER DR
P JANKE MS170
T GIOVANETTI MS236
B VAN WYK MS 389
MINNEAPOLIS MN 55421-1498

4 DIRECTOR
SANDIA NATIONAL LAB
APPLIED MECHANICS DEPT
DIV 8241
W KAWAHARA
K PERANO
D DAWSON
P NIELAN
PO BOX 969
LIVERMORE CA 94550-0096

1 BATTELLE
C R HARGREAVES
505 KNIGHT AVE
COLUMBUS OH 43201-2681

1 PACIFIC NORTHWEST LAB
M SMITH
PO BOX 999
RICHLAND WA 99352

1 LLNL
M MURPHY
PO BOX 808 L 282
LIVERMORE CA 94550

10 UNIV OF DELAWARE
CTR FOR COMPOSITE MATERIALS
J GILLESPIE
201 SPENCER LAB
NEWARK DE 19716

NO. OF COPIES ORGANIZATION

2 THE U OF TEXAS AT AUSTIN
CTR ELECTROMECHANICS
A WALLIS
J KITZMILLER
10100 BURNET RD
AUSTIN TX 78758-4497

1 AAI CORPORATION
T G STASTNY
PO BOX 126
HUNT VALLEY MD 21030-0126

1 SAIC
D DAKIN
2200 POWELL ST STE 1090
EMERYVILLE CA 94608

1 SAIC
M PALMER
2109 AIR PARK RD S E
ALBUQUERQUE NM 87106

1 SAIC
R ACEBAL
1225 JOHNSON FERRY RD STE 100
MARIETTA GA 30068

1 SAIC
G CHRYSSOMALLIS
3800 W 80TH ST STE 1090
BLOOMINGTON MN 55431

6 ALLIANT TECHSYSTEMS INC
C CANDLAND
R BECKER
L LEE
R LONG
D KAMDAR
G KASSUELKE
600 2ND ST NE
HOPKINS MN 55343-8367

1 CUSTOM ANALYTICAL ENGR
SYS INC
A ALEXANDER
13000 TENSOR LANE NE
FLINTSTONE MD 21530

NO. OF COPIES ORGANIZATION

1 NOESIS INC
1110 N GLEBE RD STE 250
ARLINGTON VA 22201-4795

1 ARROW TECH ASSO
1233 SHELBURNE RD STE D 8
SOUTH BURLINGTON VT
05403-7700

5 GEN CORP AEROJET
D PILLASCH
T COULTER
C FLYNN
D RUBAREZUL
M GREINER
1100 WEST HOLLYVALE ST
AZUSA CA 91702-0296

1 NIST
STRUCTURE & MECHANICS GRP
POLYMER DIV POLYMERS RM A209
G MCKENNA
GAITHERSBURG MD 20899

1 GENERAL DYNAMICS LAND
SYSTEM DIVISION
D BARTLE
PO BOX 1901
WARREN MI 48090

4 INSTITUTE FOR ADVANCED
TECHNOLOGY
H FAIR
P SULLIVAN
W REINECKE
I MCNAB
4030 2 W BRAKER LN
AUSTIN TX 78759

1 PM ADVANCED CONCEPTS
LORAL VOUGHT SYSTEMS
J TAYLOR MS WT 21
PO BOX 650003
DALLAS TX 76265-0003

NO. OF COPIES ORGANIZATION

2 UNITED DEFENSE LP
P PARA
G THOMASA
1107 COLEMAN AVE BOX 367
SAN JOSE CA 95103

1 MARINE CORPS SYSTEMS CMD
PM GROUND WPNS
COL R OWEN
2083 BARNETT AVE STE 315
QUANTICO VA 22134-5000

1 OFFICE OF NAVAL RES
J KELLY
800 NORTH QUINCEY ST
ARLINGTON VA 22217-5000

1 NAVSEE OJRI
G CAMPONESCHI
2351 JEFFERSON DAVIS HWY
ARLINGTON VA 22242-5160

1 USAF
WL MLS O L A HAKIM
5525 BAILEY LOOP 243E
MCCLELLAN AFB CA 55552

1 NASA LANGLEY
J MASTERS MS 389
HAMPTON VA 23662-5225

2 FAA TECH CTR
D OPLINGER AAR 431
P SHYPRYKEVICH AAR 431
ATLANTIC CITY NJ 08405

1 NASA LANGLEY RC
CC POE MS 188E
NEWPORT NEWS VA 23608

1 USAF
WL MLBC
E SHINN
2941 PST STE 1
WRIGHT PATTERSON AFB OH
45433-7750

NO. OF COPIES ORGANIZATION

4 NIST
POLYMERS DIVISION
R PARNAS
J DUNKERS
M VANLANDINGHAM
D HUNSTON
GAITHERSBURG MD 20899

1 OAK RIDGE NATIONAL LAB
A WERESZCZAK
BLDG 4515 MS 6069
PO BOX 2008
OAKRIDGE TN 37831-6064

1 COMMANDER
USA ARDEC
INDUSTRIAL ECOLOGY CTR
T SACHAR
BLDG 172
PICATINNY ARSENAL NJ
07806-5000

1 COMMANDER
USA ATCOM
AVIATION APPLIED TECH DIR
J SCHUCK
FT EUSTIS VA 23604

1 COMMANDER
USA ARDEC
AMSTA AR SRE
D YEE
PICATINNY ARSENAL NJ
07806-5000

7 COMMANDER
USA ARDEC
AMSTA AR CCH B
B KONRAD
E RIVERA
G EUSTICE
S PATEL
G WAGNECZ
R SAYER
F CHANG
BLDG 65
PICATINNY ARSENAL NJ
07806-5000

NO. OF
COPIES ORGANIZATION

1 COMMANDER
USA ARDEC
AMSTA AR QAC
T D RIGOGLIOSO
BLDG 354 M829E3 IPT
PICATINNY ARSENAL NJ
07806-5000

5 DIRECTOR
USARL
AMSRL WM MB
A ABRAHAMIAN
M BERMAN
A FRYDMAN
T LI
W MCINTOSH
E SZYMANSKI
2800 POWDER MILL RD
ADELPHI MD 20783

ABERDEEN PROVING GROUND

66 DIR USARL
AMSRL CI
AMSRL CI C
W STUREK
AMSRL CI CB
R KASTE
AMSRL CI S
A MARK
AMSRL SL B
AMSRL SL BA
AMSRL SL BE
D BELY
AMSRL WM B
A HORST
E SCHMIDT
AMSRL WM BE
G WREN
C LEVERITT
D KOOKER
AMSRL WM BC
P PLOSTINS
D LYON
J NEWILL

NO. OF
COPIES ORGANIZATION

AMSRL WM BD
S WILKERSON
R FIFER
B FORCH
R PESCE RODRIGUEZ
B RICE
AMSRL WM
D VIECHNICKI
G HAGNAUER
J MCCAULEY
AMSRL WM MA
R SHUFORD
S MCKNIGHT
L GHIORSE
AMSRL WM MB
V HARIK
J SANDS
W DRYSDALE
J BENDER
T BLANAS
T BOGETTI
R BOSSOLI
L BURTON
S CORNELISON
P DEHMER
R DOOLEY
B FINK
G GAZONAS
S GHIORSE
D GRANVILLE
D HOPKINS
C HOPPEL
D HENRY
R KASTE
M LEADORE
R LIEB
E RIGAS
D SPAGNUOLO
W SPURGEON
J TZENG
AMSRL WM MC
J BEATTY
AMSRL WM MD
W ROY
AMSRL WM T
B BURNS

NO. OF
COPIES ORGANIZATION

ABERDEEN PROVING GROUND (CONT)

AMSRL WM TA
W GILLICH
E RAPACKI
T HAVEL
AMSRL WM TC
R COATES
W DE ROSSET
AMSRL WM TD
W BRUCHEY
A D GUPTA
AMSRL WM BA
F BRANDON
W D AMICO
AMSRL WM BR
J BORNSTEIN
AMSRL WM TE
A NIILER
AMSRL WM BF
J LACETERA

INTENTIONALLY LEFT BLANK.

REPORT DOCUMENTATION PAGE

Form Approved
OMB No. 0704-0188

1. AGENCY USE ONLY *(Leave blank)*	2. REPORT DATE	3. REPORT TYPE AND DATES COVERED
	January 2000	Final, Oct 96 - Sep 97

4. TITLE AND SUBTITLE
Design of a Resistive Susceptor for Uniform Heating During Induction Bonding of Composites

5. FUNDING NUMBERS
AH42

6. AUTHOR(S)
Bruce K. Fink, Shridhar Yarlagadda,* and John W. Gillespie Jr.*

7. PERFORMING ORGANIZATION NAME(S) AND ADDRESS(ES)
U.S. Army Research Laboratory
ATTN: AMSRL-WM-MB
Aberdeen Proving Ground, MD 21005-5069

8. PERFORMING ORGANIZATION REPORT NUMBER
ARL-TR-2148

9. SPONSORING/MONITORING AGENCY NAMES(S) AND ADDRESS(ES)

10.SPONSORING/MONITORING AGENCY REPORT NUMBER

11. SUPPLEMENTARY NOTES
*University of Delaware, Newark, DE 19716

12a. DISTRIBUTION/AVAILABILITY STATEMENT
Approved for public release; distribution is unlimited.

12b. DISTRIBUTION CODE

13. ABSTRACT *(Maximum 200 words)*

A novel susceptor concept for metal-mesh susceptors, designed to achieve uniform in-plane temperatures during induction heating, is documented. The process involves redirecting eddy-current flow patterns in the resistive-mesh susceptor by specifically designed cut patterns in the mesh. A theoretical model was developed to predict heat generation in metal-mesh susceptors with any described network pattern. Initial results for cut patterns show significant changes in heating compared to an uncut mesh. Cut patterns can be optimized to reduce temperature gradients in the susceptor to within the processing window of the composite. Experimental results are presented for qualitative comparisons.

14. SUBJECT TERMS
composites, induction, alternative curing, resistive susceptor

15. NUMBER OF PAGES
36

16. PRICE CODE

17. SECURITY CLASSIFICATION OF REPORT	18. SECURITY CLASSIFICATION OF THIS PAGE	19. SECURITY CLASSIFICATION OF ABSTRACT	20. LIMITATION OF ABSTRACT
UNCLASSIFIED	UNCLASSIFIED	UNCLASSIFIED	UL

INTENTIONALLY LEFT BLANK.

USER EVALUATION SHEET/CHANGE OF ADDRESS

This Laboratory undertakes a continuing effort to improve the quality of the reports it publishes. Your comments/answers to the items/questions below will aid us in our efforts.

1. ARL Report Number/Author ARL-TR-2148 (Fink) Date of Report January 2000

2. Date Report Received _____

3. Does this report satisfy a need? (Comment on purpose, related project, or other area of interest for which the report will be used.) _____

4. Specifically, how is the report being used? (Information source, design data, procedure, source of ideas, etc.) _____

5. Has the information in this report led to any quantitative savings as far as man-hours or dollars saved, operating costs avoided, or efficiencies achieved, etc? If so, please elaborate. _____

6. General Comments. What do you think should be changed to improve future reports? (Indicate changes to organization, technical content, format, etc.) _____

CURRENT ADDRESS

_____
Organization

_____
Name E-mail Name

_____
Street or P.O. Box No.

_____
City, State, Zip Code

7. If indicating a Change of Address or Address Correction, please provide the Current or Correct address above and the Old or Incorrect address below.

OLD ADDRESS

_____
Organization

_____
Name

_____
Street or P.O. Box No.

_____
City, State, Zip Code

(Remove this sheet, fold as indicated, tape closed, and mail.)

(DO NOT STAPLE)

DEPARTMENT OF THE ARMY

OFFICIAL BUSINESS

BUSINESS REPLY MAIL
FIRST CLASS PERMIT NO 0001,APG,MD

POSTAGE WILL BE PAID BY ADDRESSEE

DIRECTOR
US ARMY RESEARCH LABORATORY
ATTN AMSRL WM MB
ABERDEEN PROVING GROUND MD 21005-5069

NO POSTAGE
NECESSARY
IF MAILED
IN THE
UNITED STATES